

PRECISION ON-BOARD ORBIT MODEL FOR ATTITUDE CONTROL OF THE ADVANCED LAND OBSERVING SATELLITE (ALOS)

Takanori Iwata

*Japan Aerospace Exploration Agency (JAXA), 2-1-1 Sengen, Tsukuba, Ibaraki 305-8505 JAPAN,
iwata.takanori@jaxa.jp*

Abstract: Star-sensor-based attitude determination system estimates spacecraft attitude with respect to the inertial coordinate system. When a satellite having the star-sensor-based attitude determination system implements geocentric pointing, it requires satellite's position information relative to the geocenter. Conventional Earth pointing satellites had carried only low-order on-board orbit models, because of their Earth-sensor-based attitude determination systems and moderate attitude accuracy requirements. The Advanced Land Observing Satellite (ALOS) that had stringent attitude control accuracy and attitude stability requirements and therefore star-sensor-based attitude determination system carried a high-order precision on-board orbit model having 15 parameters and accomplished the required accuracy by frequent updates of those parameters. This paper presents the design of the on-board orbit model and its flight results. In addition, the attitude control errors and attitude stability performance that were induced by the attitude control reference generated by the orbit model were assessed.

Keywords: Orbit Model, Orbit Propagator, Attitude Control, Attitude Stability, ALOS, Flight Experience.

1. Introduction

Advances in mission requirements result in the pursuit of more precise attitude determination and control. Because of this trend, supported by star sensors' advances, star-sensor-based attitude determination and control becomes a standard, in particular, for recent Earth observation satellites whose reference attitude is geocentric pointing. Star-sensor-based attitude determination system estimates spacecraft attitude with respect to the inertial frame. When a satellite having the star-sensor-based attitude determination system seeks geocentric pointing, it requires satellite's position information relative to the geocenter for generating an attitude control reference frame. And, accuracy and stability of the satellite position information can be a major factor for satellite's attitude control accuracy and attitude stability.

On-board orbit models are one of the approaches for giving the satellite position information. Conventional Earth pointing satellites had carried only low-order and therefore low-accuracy on-board orbit models, because of their Earth-sensor-based attitude determination systems and moderate attitude accuracy requirements. Recent Earth observation satellites having star-sensor-based attitude determination systems, such as SPOT and Envisat, carried higher-order on-board orbit models (typically 10th order) than those of conventional satellites and generated attitude control reference frames based on the orbit models [1][2]. However, as further improvement in attitude control accuracy and attitude stability is required, more precise position information is needed.

The Advanced Land Observing Satellite (ALOS) developed by the Japan Aerospace Exploration Agency (JAXA) was launched on January 24, 2006 into a sun-synchronous sub-recurrent orbit of a perigee altitude of 692 km, and has been operated successfully for 5 years since then (Fig. 1). This high-resolution satellite, whose mission includes cartography and disaster monitoring by means of global collection of high-resolution Earth images, had stringent attitude control accuracy and attitude stability requirements. Therefore, it carried and implemented a star-sensor-based attitude determination system to its flight software. It propagates a high-order precision on-board orbit

model having 15 parameters and updates it frequently, for generating a precise attitude control reference frame, instead of using its on-board GPS receiver's navigation results or a low-order on-board orbit model.

Presented in this paper are the design of the ALOS' high-order on-board orbit model and its flight data analysis. The flight data analysis includes the assessment of attitude control accuracy and attitude stability due to the on-board orbit model.

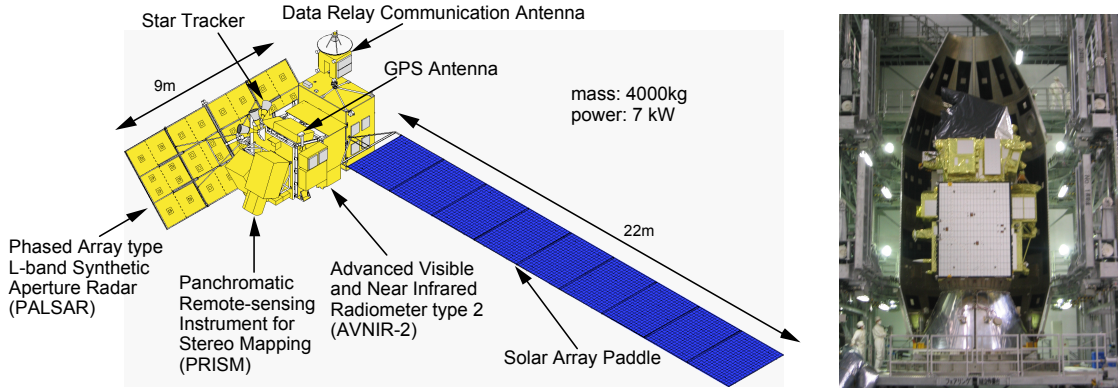


Figure 1. Advanced Land Observing Satellite (ALOS)
(Left: On-Orbit Configuration, Right: 20 Days before Launch)

2. On-Board Orbit Model

2.1. Attitude Control Reference Frame and Attitude Control Error

Earth pointing satellites require satellites' position (and velocity) information relative to the geocenter in order to generate the attitude control reference frame (*i.e.* orbit frame) to which the attitude is controlled. If the estimated position and velocity information have an error with respect to true position and velocity, the generated attitude control reference frame will have an orientation error with respect to true (*i.e.* ideal) attitude control reference frame to which the attitude is supposed to be controlled, as Fig. 2 shows. This orientation error, which this paper calls the attitude control reference frame error, causes the attitude control error. This attitude control reference frame error often becomes a major error source for the attitude control error. Note that the attitude control error consists of the attitude control reference frame error and an attitude control error with respect to the generated attitude control reference frame, and the latter consists of an attitude determination error and an attitude control residual, which is the dynamics error that attitude control could not compensate.

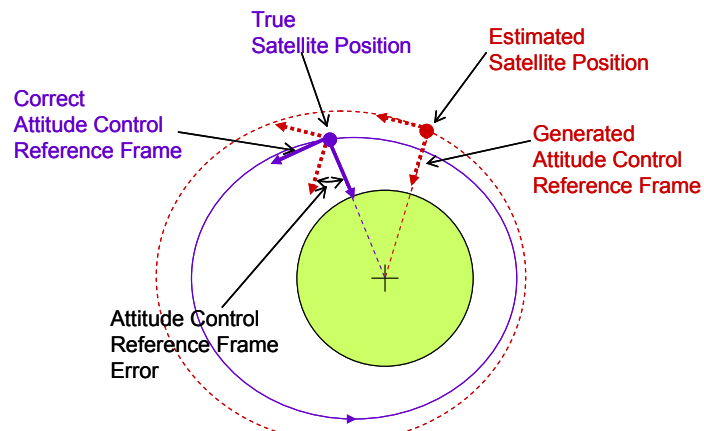


Figure 2. Satellite Position and Earth Pointing Attitude Control Reference Frame

2.2. ALOS Attitude and Orbit Control System's Approach

The ALOS Attitude and Orbit Control System (AOCS) [3] is a key subsystem in achieving the precision pointing requirement given by conflicting mission requirements: global data collection of high-resolution images, and therefore, is designed for precision. In order to accomplish precision attitude requirement broken down from the precision pointing requirement, AOCS has a newly-developed three-head precision star tracker and a newly-developed 64-bit-MPU-based high-performance attitude control computer, implements an extended-Kalman-filter-based precision attitude determination system using the star tracker and an inertial reference unit for the first time as Japanese Earth pointing satellites, and controls its attitude using this attitude estimate. Figure 3 shows a closed-loop block diagram of ALOS AOCS.

As Fig. 1 shows, AOCS calculates attitude quaternion estimates with respect to the inertial frame by an extended Kalman filter using measurement data of the star tracker and the inertial reference unit. Because the mission attitude is geocenter pointing, AOCS has to define an orbit frame representing the satellite's current position and velocity and control a difference between the satellite attitude and the orbit frame. In order to define the orbit frame, the corresponding coordinate transformation matrix (coordinate rotation) from the inertial frame to the orbit frame is necessary. To derive the coordinate transformation matrix, the satellite's current orbit information is needed.

There are two major approaches for estimating the satellite's real-time orbit information. One is an approach based on the propagation of on-board orbit models which are used in attitude and orbit control systems of conventional Earth observation satellites such as ADEOS and ADEOS-II. The other is an approach in which the satellite carries a GPS receiver and uses on-board navigation results provided by the on-board GPS receiver. The approach based on the propagation of on-board orbit models requires the ground-based estimation of parameters of the on-board orbit model and the periodic upload of them to the satellite. Despite this operational load, the on-board orbit model approach has benefits in its simplicity, stability, and robustness. Since ADEOS and ADEOS-II carried only Earth-sensor-based attitude determination systems, the generation of precise attitude control reference that ALOS requires was not necessary. Therefore, although ADEOS' and ADEOS-II's low-order on-board orbit model provided only low accuracy, the generation of orbit information by on-board orbit models itself is attractive because of its simplicity and flight heritages.

On the other hand, the generation of orbit information by GPS receiver's real-time navigation has benefits in accuracy and reduction of operational load. However, it has a risk in terms of stable continuation of the receiver's navigation. If the real-time navigation is interrupted by external causes such as interference signals or receiver's problems, the attitude control system has to suspend its attitude control and change its control mode. ALOS carries a newly-developed dual-frequency carrier-phase measuring GPS receiver. If we introduced the GPS receiver's navigation results into the ALOS' attitude control loop, it would increase a complexity of the attitude control loop and add a risk that two newly developed items of the GPS receiver and the star-tracker-based precision attitude determination system are required to realize specified function and performance of the attitude control system. In addition, if we used the orbit frame based on the GPS receiver's stand-alone navigation results, it would degrade attitude stability because of random errors of the navigation results. Therefore, we adopted the approach in which we do not introduce the GPS receiver's navigation results to the attitude control loop but implemented more precise on-board orbit model by which AOCS generates the attitude control reference frame to obtain required attitude control accuracy and stability. This function corresponds to the block denoted by Reference Attitude Generation in Fig. 3.

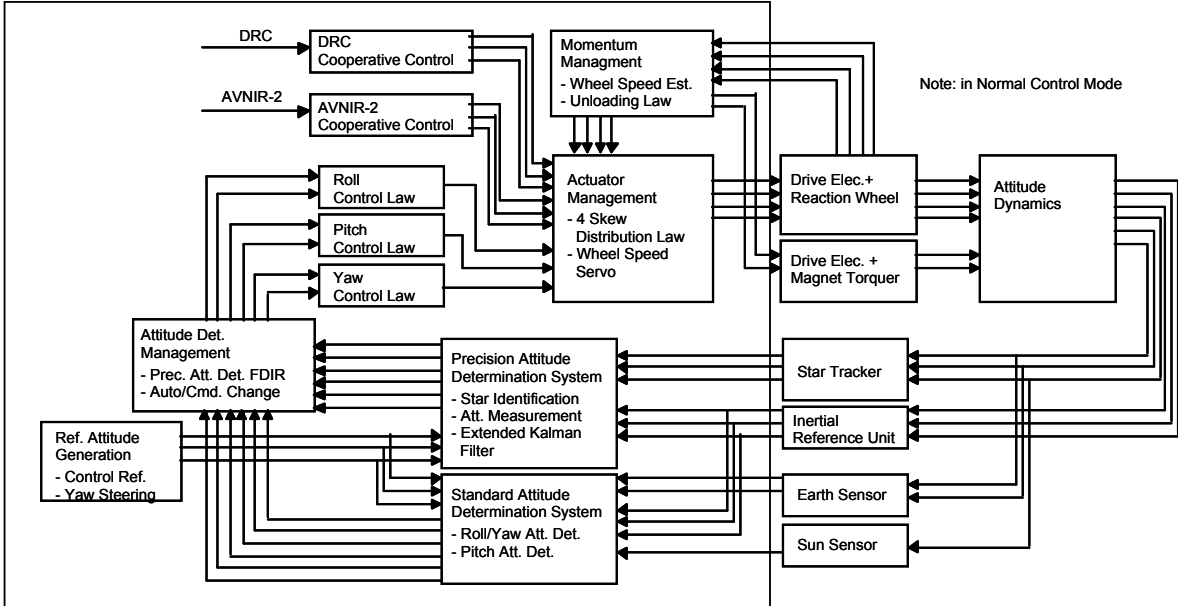


Figure 3. Closed-Loop Block Diagram of ALOS Attitude and Orbit Control System

2.3. High-Order On-Board Orbit Model

The ALOS' Attitude and Orbit Control Flight Software (ACFS) has an on-board orbit model that always calculates the satellite orbit on-board based on parameters transmitted from the ground and can derive the Earth center from the calculated orbit elements. The on-board orbit model consists of orbit elements to be estimated, constant coefficient parameters K_i determined based on a nominal orbit, and variable parameters P_i to be updated within specific intervals. In order to obtain more precise satellite orbit elements (*i.e.* satellite position and velocity) that the orbit model estimates and to reduce the attitude control reference frame's error contribution out of attitude control error, we modeled ALOS' orbit motion at 15-th order for both K_i and P_i , and propagates it on-board.

Perturbation factors taken into account are secular and short-period perturbations by the J2 term, an atmospheric drag perturbation, long-period perturbations by the non-zonal terms, and eccentricity vector rotation by the J2 and J3 terms. The ALOS' on-board orbit model is given by

$$\begin{aligned}
 a(t) &= P_1 + K_1 \cos 2\bar{\alpha} + P_{15}t \\
 e_x(t) &= P_2 + K_2 \cos 3\bar{\alpha} + K_3 \cos \bar{\alpha} + P_{13}t + K_{14} \cos [(\dot{\theta}_G - P_7)t + P_{12}] \\
 e_y(t) &= P_3 + K_2 \sin 3\bar{\alpha} + K_4 \sin \bar{\alpha} + P_{14}t + K_{15} \sin [(\dot{\theta}_G - P_7)t + P_{12}] \\
 i(t) &= P_4 + K_5 \cos 2\bar{\alpha} + K_8 \cos [2(\dot{\theta}_G - P_7)t + P_{10}] + K_{11} \sin [(\dot{\theta}_G - P_7)t + P_{11}] \\
 \Omega(t) &= P_5 + P_7t + K_6 \sin 2\bar{\alpha} + K_{10} \sin [2(\dot{\theta}_G - P_7)t + P_{10}] + K_{13} \cos [(\dot{\theta}_G - P_7)t + P_{11}] \\
 \alpha(t) &= \bar{\alpha} + K_7 \sin 2\bar{\alpha} + K_9 \sin [2(\dot{\theta}_G - P_7)t + P_{10}] + K_{12} \cos [(\dot{\theta}_G - P_7)t + P_{11}] \\
 \bar{\alpha}(t) &= P_6 + P_8t + P_9t^2 \\
 e_x(t) &= e(t) \cos \omega(t) \quad e_y(t) = e(t) \sin \omega(t) \quad \alpha(t) = \omega(t) + M(t),
 \end{aligned}$$

where t is an elapsed time from an epoch t_0 . Using these equations, the orbit elements (the semi-major axis a , the eccentricity vector e_x, e_y , the inclination i , the right ascension of ascending node Ω , and the argument of latitude α) are calculated at every control cycle (100 ms).

The constant coefficient parameters K_i of the on-board orbit model represent perturbations caused by the Earth's gravitational potential, as described below, and are pre-determined by the nominal orbit elements of the satellite:

(1) Short-period perturbation by J2 term

$$\begin{aligned} K_1 &= \frac{3}{2} J_2 \frac{a_e^2}{a} \sin^2 i & K_2 &= \frac{7}{8} J_2 \frac{a_e^2}{a^2} \sin^2 i \\ K_3 &= \frac{3}{8} J_2 \frac{a_e^2}{a^2} (4 - 5 \sin^2 i) & K_4 &= \frac{3}{8} J_2 \frac{a_e^2}{a^2} (4 - 7 \sin^2 i) \\ K_5 &= \frac{3}{4} J_2 \frac{a_e^2}{a^2} \sin i \cos i & K_6 &= \frac{3}{4} J_2 \frac{a_e^2}{a^2} \cos i \\ K_7 &= \frac{3}{8} J_2 \frac{a_e^2}{a^2} (3 - 5 \cos^2 i) \end{aligned}$$

(2) Long-period perturbation by non-zonal (2, 2) term

$$\begin{aligned} K_8 &= \frac{3}{2} \frac{n}{\dot{\theta}_G - \dot{\Omega}} \frac{a_e^2 r_{22}}{a^2} \sin i \\ K_9 &= \frac{3}{2} \frac{n}{\dot{\theta}_G - \dot{\Omega}} \frac{a_e^2 r_{22}}{a^2} (3 - 4 \cos^2 i) \\ K_{10} &= \frac{3}{2} \frac{n}{\dot{\theta}_G - \dot{\Omega}} \frac{a_e^2 r_{22}}{a^2} \cos i \end{aligned}$$

(3) Long-period perturbation by non-zonal (3, 1) term

$$\begin{aligned} K_{11} &= -\frac{15}{4} \frac{n}{\dot{\theta}_G - \dot{\Omega}} \frac{a_e^4 r_{41}}{a^4} \cos i \left(1 - \frac{7}{4} \sin^2 i \right) \\ K_{12} &= -\frac{15}{4} \frac{n}{\dot{\theta}_G - \dot{\Omega}} \frac{a_e^4 r_{41}}{a^4} \frac{\cos i}{\sin i} \left(1 + \frac{29}{4} \sin^2 i - \frac{49}{2} \sin^2 i \cos^2 i \right) \\ K_{13} &= \frac{15}{4} \frac{n}{\dot{\theta}_G - \dot{\Omega}} \frac{a_e^4 r_{41}}{a^4 \sin i} \left(1 - \frac{1}{4} \sin^2 i - 7 \sin^2 i \cos^2 i \right) \end{aligned}$$

(4) Long-period perturbation by non-zonal (4, 1) term

$$\begin{aligned} K_{14} &= -\frac{3}{2} \frac{n}{\dot{\theta}_G - \dot{\Omega}} \frac{a_e^3 r_{31}}{a^3} \cos i \left(1 - \frac{15}{4} \sin^2 i \right) \\ K_{15} &= \frac{3}{2} \frac{n}{\dot{\theta}_G - \dot{\Omega}} \frac{a_e^3 r_{31}}{a^3} \left(-1 + \frac{5}{4} \sin^2 i \right) \end{aligned}$$

Physical meaning of each parameter is summarized in Table 1. K_1, \dots, K_7 represent the short-period perturbation caused by the J2 term. K_8, \dots, K_{10} represent the long-period perturbation caused by the non-zonal (2,2) term, K_{11}, \dots, K_{13} represent the long-period perturbation caused by the non-zonal (4,1) term, and K_{14} and K_{15} represent the long-period perturbation caused by the non-zonal (3,1) term.

On the other hand, the variable parameters P_i given below are updated at the regular intervals (once per a few days) corresponding to an acceptable orbit estimation error. Physical meaning of each parameter P_i is summarized in Table 3.

(1) Mean orbit elements at the epoch

$$\begin{aligned} P_1 &= a(t_0) & P_2 &= e_x(t_0) \\ P_3 &= e_y(t_0) & P_4 &= i(t_0) \\ P_5 &= \Omega(t_0) & P_6 &= \alpha(t_0) = \omega(t_0) + M(t_0) \end{aligned}$$

Table 1. Constant Coefficient Parameters K_i

K_i	Perturbation Factor
K_1	Short-Period Perturbation of a by J_2 term (Period: 2α)
K_2	Short-Period Perturbation of e by J_2 term (Period: 3α)
K_3	Short-Period Perturbation of e_x by J_2 term (Period: α)
K_4	Short-Period Perturbation of e_y by J_2 term (Period: α)
K_5	Short-Period Perturbation of i by J_2 term (Period: 2α)
K_6	Short-Period Perturbation of Ω by J_2 term (Period: 2α)
K_7	Short-Period Perturbation of α by J_2 term (Period: 2α)
K_8	Long-Period Perturbation of i by (C_{22}, S_{22}) term (Period: $2(\dot{\Omega} - \dot{\theta})$)
K_9	Long-Period Perturbation of Ω by (C_{22}, S_{22}) term (Period: $2(\dot{\Omega} - \dot{\theta})$)
K_{10}	Long-Period Perturbation of α by (C_{22}, S_{22}) term (Period: $2(\dot{\Omega} - \dot{\theta})$)
K_{11}	Long-Period Perturbation of i by (C_{41}, S_{41}) term (Period: $\dot{\Omega} - \dot{\theta}$)
K_{12}	Long-Period Perturbation of Ω by (C_{41}, S_{41}) term (Period: $\dot{\Omega} - \dot{\theta}$)
K_{13}	Long-Period Perturbation of α by (C_{41}, S_{41}) term (Period: $\dot{\Omega} - \dot{\theta}$)
K_{14}	Long-Period Perturbation of e_x by (C_{31}, S_{31}) term (Period: $\dot{\Omega} - \dot{\theta}$)
K_{15}	Long-Period Perturbation of e_y by (C_{31}, S_{31}) term (Period: $\dot{\Omega} - \dot{\theta}$)

Table 2. Variable Parameters P_i

P_i	Factor
P_1	Semi-Major Axis of Mean Orbit Elements at Epoch, a
P_2	Eccentricity Vector of Mean Orbit Elements at Epoch, e_x
P_3	Eccentricity Vector of Mean Orbit Elements at Epoch, e_y
P_4	Inclination of Mean Orbit Elements at Epoch, i
P_5	Right Ascension of Ascending Node of Mean Orbit Elements at Epoch, Ω
P_6	Argument of Latitude of Mean Orbit Elements at Epoch, α
P_7	Rate of Change of Right Ascension of Ascending Node, $d\Omega/dt$
P_8	Rate of Change of Argument of Latitude, $d\alpha/dt$
P_9	Rate of Change of Rate of Change of Argument of Latitude, $d^2\alpha/dt^2$
P_{10}	$2\Omega - 2\theta_G - \theta_{22}$ at Epoch
P_{11}	$\Omega - \theta_G - \theta_{41}$ at Epoch
P_{12}	$\Omega - \theta_G - \theta_{31}$ at Epoch
P_{13}	Rate of Change of Mean Eccentricity Vector, de_x/dt
P_{14}	Rate of Change of Mean Eccentricity Vector, de_y/dt
P_{15}	Reduction Rate of Semi-Major Axis, da/dt

(2) Rate of change in right ascension of ascending node and argument of latitude by J2term secular perturbation

$$P_7 = \frac{d\Omega}{dt} \quad P_8 = \frac{d\alpha}{dt}$$

(3) Rate of change in rate of change of argument of latitude by atmospheric drag

$$P_9 = \frac{d^2\alpha}{dt^2}$$

(4) Argument of non-zonal (2, 2), (4, 1), and (3, 1) terms at the epoch

$$\begin{aligned} P_{10} &= 2\Omega(t_0) - 2\theta_G(t_0) - \theta_{22}(t_0) \\ P_{11} &= \Omega(t_0) - \theta_G(t_0) - \theta_{41}(t_0) \\ P_{12} &= \Omega(t_0) - \theta_G(t_0) - \theta_{31}(t_0) \end{aligned}$$

(5) Rate of change in eccentricity vector by J2 and J3 terms

$$P_{13} = \frac{de_x}{dt} \quad P_{14} = \frac{de_y}{dt}$$

(6) Rate of change in semi-major axis by atmospheric drag

$$P_{15} = \frac{da}{dt}$$

P_1, \dots, P_6 are mean orbit elements at the epoch. P_7 and P_8 represent the secular perturbation caused by the J2 term, P_9 and P_{15} represent the atmospheric drag perturbation, and P_{13} and P_{14} represent the change of the mean eccentricity vector.

The original model is defined for the true-of-date inertial frame. However, because the on-board attitude control system performs the attitude determination and control with respect to the J2000.0 inertial frame, we use the model and parameters for the J2000.0 inertial frame in operations.

2.4. Background

The basic concept of on-board orbit models lies on analytical solutions of the general perturbation technique. Early works on the analytical solutions are found in Kozai's method based on Lagrange planetary equations [4] and in Brouwer's method based on Hamiltonian planetary equations [5] with the form [6]:

$$\begin{aligned} a &= \bar{a} + \Delta a_{LP} + \Delta a_{SP} \\ e &= e_0 + \Delta e_{LP} + \Delta e_{SP} \\ i &= i_0 + \Delta i_{LP} + \Delta i_{SP} \\ \omega &= \omega_0 + \dot{\omega}\Delta t + \Delta\omega_{LP} + \Delta\omega_{SP} \\ \Omega &= \Omega_0 + \dot{\Omega}\Delta t + \Delta\Omega_{LP} + \Delta\Omega_{SP} \\ M &= M_0 + \bar{n}\Delta t + \Delta M_{LP} + \Delta M_{SP} \end{aligned}$$

The original works did not take into account atmospheric drag, but later, various extensions to their methods have been published [6]. The analytical solutions are also extended to operational applications under the names: orbit propagators, orbit propagation models, or orbit models. Typical and sophisticated examples for ground-based orbit propagation include the Simplified General Perturbations 4 (SGP4) [7][8] that U. S. Air Force and NORAD use and the Position Partials and Time 2 (PPT2) [9] that U. S. Navy uses.

Orbit models based on analytical solutions are also used in spacecraft's on-board software. Japanese Earth observation satellites ADEOS and ADEOS-II used a low-order on-board orbit model of a form

$$x(t) = x_0 + \dot{x}_0 t, \quad x = a, e, \Omega, \omega, i, M,$$

for adjusting sun and Earth sensors measurements and for counting an orbit timer. French Earth observation satellites SPOT used an on-board orbit model with

$$K_{11}, \dots, K_{15} = 0$$

in the on-board orbit model described in Section 2.3 and updated P_1, \dots, P_{10} for pointing Earth center [1]. Another European Earth observation satellite Evnisat used a similar 10th order model having a different form [2]. The full-order (*i.e.* 15th-order) model presented in Section 2.3 was originally developed and used for a Japanese optical intersatellite communication satellite OICETS to computate its optical antenna's pointing direction for intersatellite communication. The same full-order orbit model in Section 2.3 was implemented from its development stage to a Japanese high-resolution Earth observation satellite ALOS. But, the 10th order setting with

$$K_{11}, \dots, K_{15} = 0$$

and variable P_1, \dots, P_{10} in the first 9 months after the launch. Then, on October 31, 2006, the full-order (*i.e.* 15th-order) operation with non-zero values for all 15 constant coefficient parameters and all 15 variable parameters was started and has been continued.

2.5. Parameter Estimation and Update Frequency

The JAXA's orbit dynamics system calculates orbit determination values at regular basis from measurements of range and range-rate, and obtains orbit prediction values by propagating the orbit determination values into the future. The update parameters of the on-board orbit model are estimated by least-square-method-based model-fitting of the orbit prediction values for the period to which the parameters are applied (*i.e.*, the period until the next update).

Error sources (call on-board orbit model estimation error) between orbit (position and velocity) estimated by the on-board orbit model and true satellite orbit (position and velocity) are the following three:

- Orbit model error,
- Orbit determination error, and
- Orbit prediction error.

Upon the ALOS' development, a trade-off of orbit model, model order, and parameter update frequency was performed in the point of view whether estimation error (attitude control reference frame error) of the on-board orbit model would meet the allocated budget of the attitude control error requirement. As a result, the orbit model errors are 0.700 km for along-track position, 0.221 km for cross-track position, 0.316 km for radial position, 0.34 km/s for along-track velocity, 0.27 km/s for cross-track velocity, and 0.54 m/s for radial velocity (Table 3), for the condition of a 3 day interval update, a nominal solar activity, and the original on-board orbit model at the launch (*i.e.*, $K_{11}, \dots, K_{15} = 0$ and $P_{11}, \dots, P_{15} = 0$ equivalent to that of SPOT). These are equivalent to the attitude control error of 0.0018 deg (roll), 0.0057 deg (pitch), and 0.0021 deg (yaw), which indicate sufficient accuracy as an on-board orbit model. Further, the on-board orbit model estimation error that includes the orbit determination error and the orbit prediction error is 3.78 km for the position error of the along-track direction (Table 4) in which the orbit prediction error is dominantly large, compared with other errors. This is equivalent to the pitch-axis attitude control error of 0.031 deg, which gives a sufficient margin to the attitude control error budget of 0.095 deg (3σ).

The accuracy study revealed that the attitude control accuracy requirement would be fully satisfied if the update period of the variable parameters was less than 3 days and the maximum orbit propagation time on-board (elapsed time since an epoch) was less than 84 hours. Therefore, the orbit determination is performed on Monday, Tuesday, and Thursday, and the update parameters of the orbit model whose epochs are Tuesday UT0, Thursday UT0, and Saturday UT0 are transmitted to the satellite on Tuesday, Thursday, and Saturday, respectively. This update cycle is summarized in Table 5. If the solar activity becomes maximum, however, the update frequency may have to be increased to one day interval at maximum.

Table 3. On-Board Orbit Model Error

Orbit Model Error		Orbit Model Error	
Position Error		Velocity Error	
Along Track	0.700km	0.34m/s	⇒
Cross Track	0.221km	0.27m/s	
Radial	0.316km	0.54m/s	

Orbit Model Error	
Attitude Control Error	
Roll	0.0018deg
Pitch	0.0057deg
Yaw	0.0021deg

Table 4. Orbit Model Estimation Error and Attitude Control Reference Frame Error

Along Track		Pitch	
Each Error	Orbit Model Estimation Error	Attitude Control Error	Requirement
Orbit Model Error	0.700km	3.78km	< 0.095deg
Orbit Determination Error	3.69km		
Orbit Prediction Error			
Frame Transformation Error	0.4km		

Table 5. On-Board Orbit Model Update Cycle

Orbit Determination	\Rightarrow	Orbit Model Epoch	\Rightarrow	Transmission to Satellite
Monday	\Rightarrow	Tuesday UT0	\Rightarrow	Tuesday
Tuesday	\Rightarrow	Thursday UT0	\Rightarrow	Thursday
Thursday	\Rightarrow	Saturday UT0	\Rightarrow	Saturday

2.6. Generation of Attitude Control Reference Frame

The attitude control reference frame is generated by the following process. First, we convert orbit elements $[a \ e \ f \ \Omega \ i \ \omega]$ of an on-board orbit model into an equivalent position and velocity vectors in the J2000.0 inertial frame.

$$\vec{r}_{pf} = \begin{bmatrix} r \cos f \\ r \sin f \\ 0 \end{bmatrix} \quad \vec{v}_{pf} = \sqrt{\frac{\mu}{a(1-e^2)}} \begin{bmatrix} -\sin f \\ e + \cos f \\ 0 \end{bmatrix} \quad r = \frac{a(1-e^2)}{1+e \cos f}$$

$$\vec{r}_o = T_{pf}^{gi} \vec{r}_{pf} \quad \vec{v}_o = T_{pf}^{gi} \vec{v}_{pf}$$

$$T_{pf}^{gi} = \begin{bmatrix} \cos \Omega \cos \omega - \sin \Omega \sin \omega \cos i & -\cos \Omega \sin \omega - \sin \Omega \cos \omega \cos i & \sin \Omega \sin i \\ \sin \Omega \cos \omega + \cos \Omega \sin \omega \cos i & -\sin \Omega \sin \omega + \cos \Omega \cos \omega \cos i & -\cos \Omega \sin i \\ \sin \omega \sin i & \cos \omega \sin i & \cos i \end{bmatrix}$$

Then, a direction cosine matrix is derived from the position and velocity vectors as follows:

$$\vec{e}_{z0} = \frac{-\vec{r}_o}{|\vec{r}_o|}, \quad \vec{e}_{y0} = \frac{\vec{v}_o \times \vec{r}_o}{|\vec{v}_o \times \vec{r}_o|}, \quad \vec{e}_{x0} = \vec{e}_{y0} \times \vec{e}_{z0}, \quad T_{io} = [\vec{e}_{x0} \quad \vec{e}_{y0} \quad \vec{e}_{z0}]^T.$$

This direction cosine matrix is converted into a quaternion \vec{q}_{io} representing attitude rotation from the inertial frame to the estimated orbit frame specified by the on-board orbit model.

$$T_{4 \times 4} = \begin{bmatrix} T_{io} & 0 \\ 0 & tr(T_{io}) \end{bmatrix}, \quad T_{4 \times 4} \Rightarrow \dots \Rightarrow \vec{q}_{io}.$$

Given an attitude estimate quaternion \vec{q}_{ib} representing satellite attitude with respect to the inertial frame, we obtain an attitude error quaternion \vec{q}_{ob} representing attitude rotation from the estimated orbit frame to the satellite body frame by the following quaternion manipulation:

$$\vec{q}_{ob} = \begin{bmatrix} q_{ib,4} & q_{ib,3} & -q_{ib,2} & q_{ib,1} \\ -q_{ib,3} & q_{ib,4} & q_{ib,1} & q_{ib,2} \\ q_{ib,2} & -q_{ib,1} & q_{ib,4} & q_{ib,3} \\ -q_{ib,1} & -q_{ib,2} & -q_{ib,3} & q_{ib,4} \end{bmatrix} \vec{q}_{oi},$$

where

$$\vec{q}_{oi} = [-q_{io,1} \quad -q_{io,2} \quad -q_{io,3} \quad q_{io,4}]^T, \quad \vec{q}_{ib} = [q_{ib,1} \quad q_{ib,2} \quad q_{ib,3} \quad q_{ib,4}]^T.$$

Euler angles are calculated from this attitude error quaternion as follows (in this paper, 2-1-3 rotations are used):

$$\begin{aligned}\phi &= -\sin^{-1} [2(q_{ob,2}q_{ob,3} - q_{ob,1}q_{ob,4})] \\ \theta &= \tan^{-1} \left[\frac{2(q_{ob,1}q_{ob,3} + q_{ob,2}q_{ob,4})}{1 - 2(q_{ob,1}^2 + q_{ob,2}^2)} \right], \\ \psi &= \tan^{-1} \left[\frac{2(q_{ob,1}q_{ob,2} + q_{ob,3}q_{ob,4})}{1 - 2(q_{ob,1}^2 + q_{ob,3}^2)} \right].\end{aligned}$$

For these Euler angles, ALOS executes 3-axis independent attitude control.

The same process described above was applied to the calculation of the attitude control reference error (one factor of attitude control error) induced by an on-board orbit model. It was applied not only to the transformation of orbit elements obtained from an on-board orbit model telemetry but also to the transformation of a quaternion corresponding to a precision orbit estimate used as a true value. The attitude control reference error induced by the on-board orbit model was obtained by calculating the error quaternion between the quaternion derived from the on-board orbit model telemetry and the quaternion derived from the precision orbit estimate and then transforming it to the Euler angles.

3. Flight Data Analysis

3.1. Behavior of On-Board Orbit Model

ALOS AOCS downlinks to the ground 24-hour-length 1-sec-interval orbit elements out of full-rate (10 Hz) on-board computation results of the on-board orbit model as a part of low-speed mission data. This section compares the on-board orbit model telemetries that AOCS actually propagated on-board with the precision orbit estimates that the ground-based precision orbit determination system (GUTS) computed from dual-frequency measurements of the ALOS GPS receiver. The accuracy of the GUTS-generated ALOS precision orbit estimates is 0.37 m (3σ) for distance error [4] and is far better than the estimation accuracy of the on-board orbit model. Therefore, the succeeding analysis of the on-board orbit model's propagation results assumes that the GUTS precision orbit estimates represent true values.

A typical one-day propagation result (solid line) of the on-board orbit model is shown with corresponding orbit elements derived from the GUTS precision orbit estimates, in Fig. 4. This shows the behavior of the modeled perturbation terms and verifies that they represent a majority of the actual orbit motion. In Fig. 4, the difference between the orbit model's orbit elements and the true orbit elements is very small and hardly distinguishable. Therefore, the difference of each orbit element is calculated and shown in Fig. 5. This assessment indicates that the accuracy of the on-board orbit model is less than ± 100 m for semi-major axis, $\pm 2e-5$ for eccentricity vector, ± 0.001 deg for inclination, ± 0.001 deg for right ascension of ascending node, and ± 0.05 deg for argument of latitude. In operations, the variable parameters of the on-board orbit model were updated at about UT8 hour. Therefore, the first one third of the profiles represents data after nearly three day propagation. However, the estimation error of the on-board orbit model did not show a significant change before and after the update. This is mainly due to a very quiet solar activity of those days.

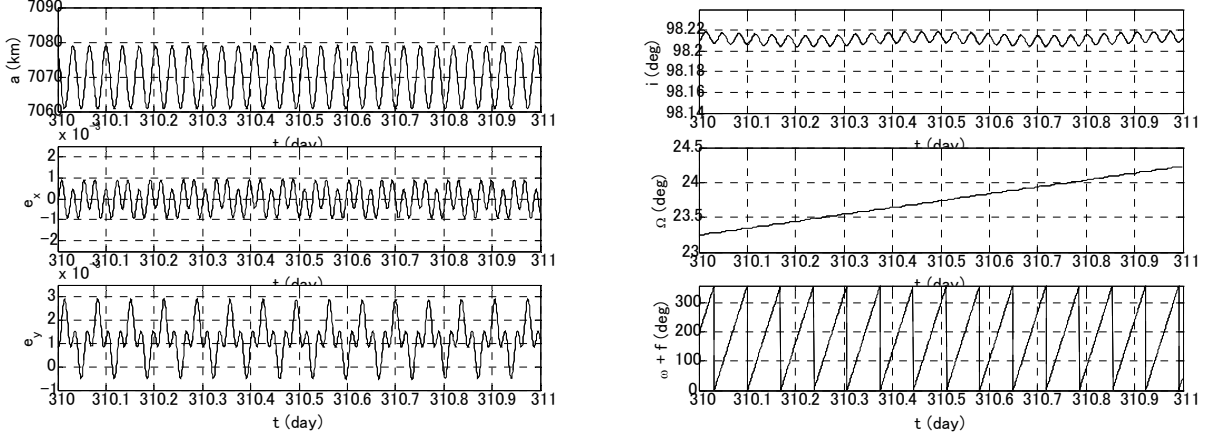


Figure 4. On-Board Orbit Model Flight Data and True Orbit Elements (UT0:00 to 24:00, November 7, 2006, Solid Line: On-Board Orbit Model, Broken Line: True Orbit Elements)

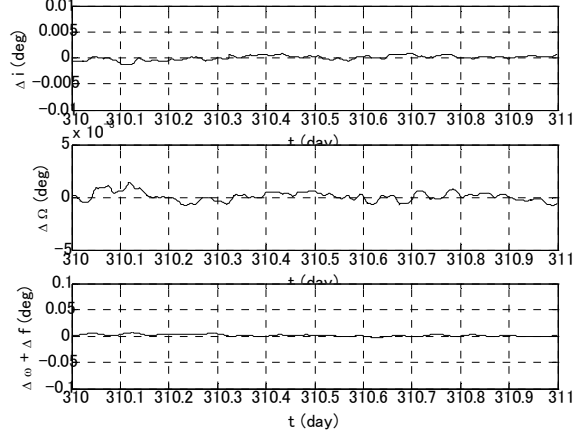
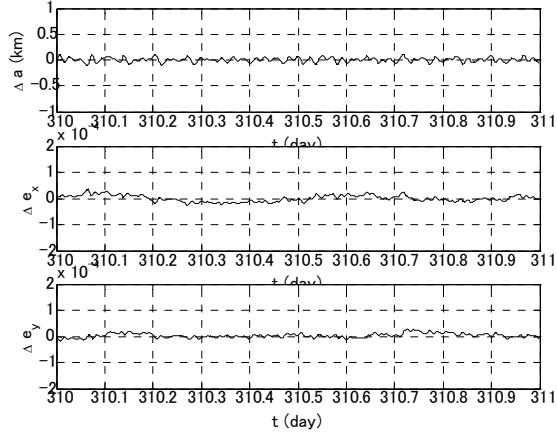


Figure 5. Orbit Element Error Profile of On-Board Orbit Model Flight Data (UT0:00 to 24:00, November 7, 2006)

3.2. Assessment of Attitude Control Accuracy and Attitude Stability

The same on-board orbit model flight data and GUTS precision orbit estimates assessed in Section 3.1 are converted to the orbit frames they define and the rotational component error between the two orbit frames is transformed to Euler angles. This set of Euler angles represents the attitude control reference frame error caused by the on-board orbit model estimation error and constitutes a part of the attitude control error. The result is shown in Fig. 6. Roll and yaw angle errors of ± 0.002 deg, and pitch angle error of ± 0.01 deg are obtained. Further, the obtained attitude error profiles are used to calculate attitude stability. As Fig. 7 shows, the attitude stability degradation induced by the on-board orbit model stays within 2×10^{-5} deg/sec.

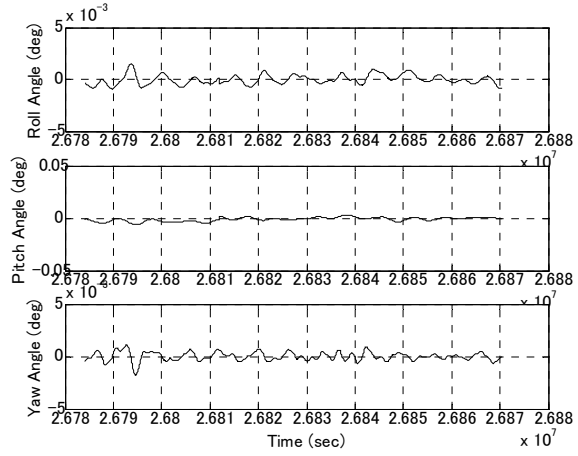


Figure 6. Attitude Control Reference Frame Error: Attitude Control Error due to On-Board Orbit Model (UT0:00 to 24:00, November 7, 2006)

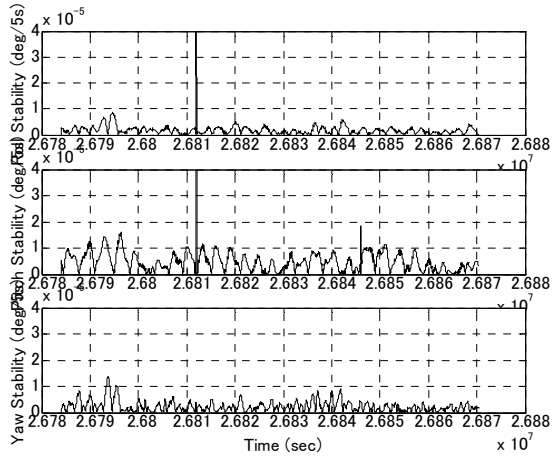


Figure 7. Attitude Control Reference Frame Stability: Attitude Stability due to On-Board Orbit Model (UT0:00 to 24:00, November 7, 2006)

3.3. 15th-Order On-Board Orbit Model

On October 31, 2006, we uploaded a set of values having full degrees-of-freedom (*i.e.* 15th order) for both constant coefficient parameters and variable parameters of the on-board orbit model and started the operation that would exploit full-capability of the on-board software to which the 15th-order orbit model had been implemented from the beginning. The on-board orbit model error before and after the 15th-order setting is shown in Fig. 8, while the attitude control error due to the on-board orbit model error (*i.e.* the attitude control reference frame error) and the attitude stability due to the on-board orbit model error are shown in Figs. 9 and 10. Spikes slightly before 303.5 days in the plots represent the execution of the 15th-order setting. Figure 8 suggests that the 15th-order operation reduced amplitudes of the periodic terms expressed by the parameters of 11th and higher. The attitude control error profile and the attitude stability profile demonstrates even more significant improvements.

More quantitative analysis was performed to assess the improvements of the attitude control error and the attitude stability upon the 15th-order setting, and the results were summarized in Table 6. For three day data before and after the 15th-order setting, the attitude control error and the attitude stability due to the on-board orbit model were calculated and stochastically processed. As Table 6 shows, the attitude control error was reduced and the attitude stability was improved by 30 to 50 %.

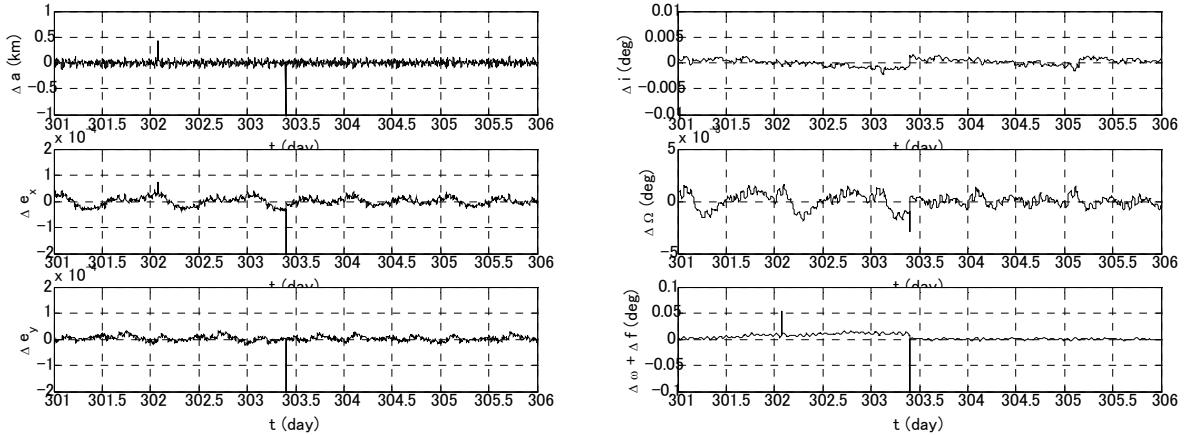


Figure 8. On-Board Orbit Model Error before and after 15th-Order Setting (October 29 to November 2, 2006)

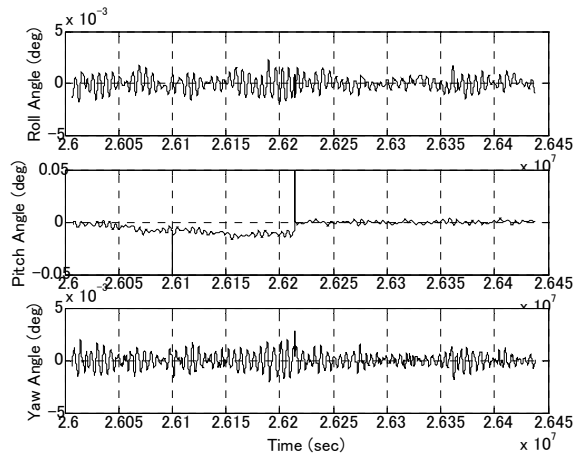


Figure 9. Attitude Control Error due to On-Board Orbit Model Error before and after 15th-Order Setting (October 29 to November 2, 2006)

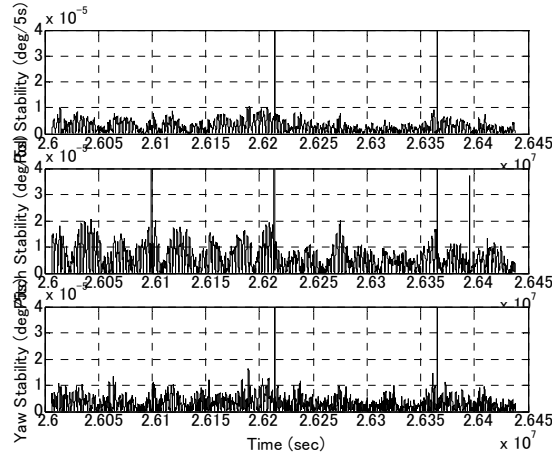


Figure 10. Attitude Stability due to On-Board Orbit Model Error before and after 15th-Order Setting (October 29 to November 2, 2006)

Table 6. Summary of Attitude Control Error and Attitude Stability before and after 15th-Order Setting (October 29 to November 2, 2006)

		Before 15th-Order Setting	After 15th-Order Setting
Evaluated Data		October 14 to 16, 2006	November 4 to 6, 2006
Attitude Control Error (deg, 3σ)	Roll	0.0025	0.0013
	Pitch	0.0104	0.0075
	Yaw	0.0024	0.0012
Attitude Stability (deg/5s, 3σ)	Roll	1.407e-5	0.756e-5
	Pitch	6.882e-5	2.020e-5
	Yaw	1.568e-5	0.985e-5

4. Conclusions

The satellites that perform precise Earth-pointing control by precision attitude determination system using a star tracker require the generation of precise attitude control reference frame. As the Advanced Land Observing Satellite (ALOS) mission requires more precise attitude control accuracy and attitude stability, we implemented a 15th-order precision on-board orbit model and updated the model relatively frequently and met the accuracy requirement. Flight data analysis showed that the 15th-order orbit model estimated most part of the ALOS' orbit motion and obtained the improvement of 30 to 50 % over the initial 10th-order setting.

5. References

- [1] Garcia-Julian, G. and Merino, M., "EPS/METOP Technical Note on Orbit Prediction", GMV-EPSFDS-TN-002, GMV S.A., Spain, 1997.
- [2] Riant, P., Val Serra, S., Fragnol, D., and Desire, P. "A Star Sensor Based AOCS for Envisat", Proceedings of 2nd ESA International Conference on GNC, ESA ESTEC, Noordwijk, Netherland, 1994.
- [3] Iwata, T., et al., "Precision Attitude and Orbit Control System for the Advanced Land Observing Satellite (ALOS)", AIAA Guidance, Navigation, and Control Conference, AIAA-2003-5783, Austin, U.S.A., 2003.
- [4] Kozai, Y., "The Motion of a Close Earth Satellite", The Astronomical Journal, Vol. 64, No. 1274, pp. 367-377, 1959.
- [5] Brouwer, D., "Solution of the Problem of Artificial Satellite Theory without Drag", The Astronomical Journal, Vol. 64, No. 1274, pp. 378-396, 1959.
- [6] Vallado, D., "Fundamentals of Astrodynamics, 3rd Edition", Microcosm Press, 2007.
- [7] Hoots, F. R., Roehrich, R. L., and Kelso, T. S., "Models for Propagation of NORAD Element Sets", Spacetrack Report No. 3, 1988.
- [8] Fonte, D. J., et al., "Comparison of Orbit Propagators in the Research and Development Goddard Trajectory Determination System", Proceedings of the AAS/AIAA Astrodynamics Conference, AAS 95-431, pp. 1949-1966, 1995.
- [9] Schumacher, P. W. Jr., and Glover, R. A., "Analytic Orbit Model for U. S. Naval Space Surveillance: an Overview", Proceedings of the AAS/AIAA Astrodynamics Conference, AAS 95-427, pp. 1893-1966, 1912.